ELSEVIER

1 May 1997

OPTICS COMMUNICATIONS

Optics Communications 137 (1997) 427–436

Full length article

Passive fiber ring flip-flop memory based on polarization dynamics

Jorge García-Mateos [a,1], Fernando Canal [a], Marc Haelterman [b,2]

[a] *Departament de Teoria del Senyal i Comunicacions, Universitat Politècnica de Catalunya, Campus Nord, c / Gran Capità s / n, E-08034 Barcelona, Spain*

[b] *Service d'Optique et Acoustique, Université Libre de Bruxelles, CP 194 / 5, 50, av. F.D. Roosvelt, B-1050 Bruxelles, Belgium*

Received 5 February 1996; revised 5 November 1996; accepted 5 December 1996

Abstract

Passive fiber ring resonators synchronously pumped by cw trains of ultrashort pulses are shown to exhibit polarization symmetry breaking. Application of this feature to all-optical storage is considered. The proposed storage device operates in the flip-flop mode which makes possible all-optical writing and erasing operations on individual bits. Numerical simulations suggest that a storage capacity of the order of thousand bits could be attainable at bit rates of hundreds of Gb/s with a maximum information processing rate of several Gb/s.

1. Introduction

Optical storage devices are essential elements of future ultra-high bit-rate fiber communication systems in which they will find applications to various vital functions. For instance, they will be used as buffers in slotted time-division-multiplexed networks where packets of data must be stored during clock recovery or rate conversion operations. In order to be compatible with fiber links bandwidth, data storage should ideally be performed all-optically. Pulse pattern storage has been demonstrated in various fiber loop devices [1–4]. These devices are based on regenerative loops [1,2] or mode-locked fiber-ring laser configurations [3,4]. They involve various pulse control techniques in order to provide timing stability of the bit patterns. Most of these stabilization techniques are based on electro-optic modulation which limits the bit rates to a few tens of Gb/s. Moreover, erasing the data in these storage fiber loops requires switching off the system electro-optically. Individual bit addressing is therefore impossible, which considerably restricts the functionality of the devices.

In the present communication, we investigate the possibility of developing a new type of all-optical fiber loop storage devices. These devices consist of simple nonlinear passive fiber ring resonators synchronously and coherently pumped by a cw mode-locked train of ultrashort pulses. It is well known that these systems exhibit rich nonlinear dynamics involving, in particular, optical bistability and period-doubling instabilities [5]. Optical bistability is a feature which is naturally suited for applications to optical storage [6]. However, erasing the data in an optical bistable element requires to switch off the holding beam and is therefore not practical. Several solutions were proposed in the literature to overcome this difficulty. On one hand, one finds double-beam ring cavities [7,8] or Fabry-Pérot [9] configurations. Besides optical bistability, these devices exhibit a pitchfork bifurcation which makes possible set-reset flip-flop operations [10,11]. On the other hand, some authors have suggested the use of the polarization of the electromagnetic field as information carrier and have developed bistable elements based on polarization dynamics [12–14]. Hybrid bistable devices as well as Kerr-type Fabry-Pérot resonators based on this principle have been suggested and studied experimentally [13]. These devices are based on bulk optics technology. They then require high nonlinear index changes, which can only be provided by slow physical processes such as thermally induced

[1] E-mail: mateos@voltor.upc.es.

[2] E-mail: mhaelter@ulb.ac.be.

PII S0030-4018(96)00784-5

Kerr-type nonlinearity [13,14]. Moreover, a high capacity memory based on this technology requires the integration of a large number of bistable elements on the same support, each of the elements being addressed individually by a separate laser beam in a way analogous to what is proposed by McDonald et al. [15] for the so-called spatial solitary-wave bistable memory. Such massive parallel addressing requires rather complex technological developments. In opposition to this, the use of optical silica fibers as nonlinear media with synchronous pulsed excitation makes possible the realization of high capacity storage with a single fiber loop.

In a recent paper, Haelterman et al. [17] have studied the polarization dynamics of nonlinear dispersive ring cavities. They have shown in particular, by use of a mean-field approach to the problem, that these devices exhibit a polarization symmetry-breaking characterized by a pitchfork bifurcation analogous to that observed in the above mentioned double-beam nonlinear Fabry-Pérot resonator. As in that latter case, this feature can be applied to the development of a set-reset flip-flop all-optical fiber loop memory. Our communication aims at presenting the results of a preliminary investigation of such a storage device. The paper is organized as follows: In Section 2, the device and the mathematical model used to its description are presented. In Section 3 we briefly analyze numerically the dynamics of the polarization symmetry-breaking bifurcation in the synchronous pulsed regime including dispersion effects. A detailed analysis of the set-reset flip-flop operation mode in the synchronous pulsed regime is then given. Section 4 presents the result of numerical simulations of basic storage and switching operations on pseudo-random bit packets. Finally, Section 5 is devoted to our conclusions in which we discuss, in particular, the practicality of the proposed device.

2. Device and theoretical model

The fiber loop storage device is schematically depicted in Fig. 1. It consists of a ring cavity made of a single-mode dual-polarization passive fiber. Two couplers provide input and output ports for both the pump and the signal. The fiber ring is coherently and synchronously pumped through coupler 1 by a high repetition rate cw mode-locked pulse train. The cavity round-trip time t_R is a multiple of the period t_S of this pump wave. Each pulse of the periodic pump wave constitutes a bit of the optical memory. Synchronous pumping insures timing stability of these bits and thus no active stabilization elements are needed in the cavity. The second coupler provides the signal input port through which trigger pulses are launched in the cavity to write and erase the bit patterns. The principle of operation of the triggering is described in Section 3.

For the sake of simplicity, we assume that the fiber birefringence is sufficiently low to be neglected in the model. We also assume that the couplers are polarization insensitive. We shall see in Section 4 that anisotropy does not modify the qualitative behavior described from this model provided that it is small. In terms of the circular polarization components $E_{\pm} = (E_x \pm iE_y)/(2)^{1/2}$, the propagation of the electromagnetic field during the nth round trip in the fiber cavity is ruled by the incoherently coupled nonlinear Schrödinger (NLS) equations [18]:

$$\frac{\partial E_{\pm}^n}{\partial Z} = -\frac{i}{2}\frac{\partial^2 E_{\pm}^n}{\partial T^2} + i\left(\tfrac{1}{3}\left|E_{\pm}^n\right|^2 + \tfrac{2}{3}\left|E_{\mp}^n\right|^2\right)E_{\pm}^n, \qquad (1)$$

where we have used the following dimensionless variables: $Z = z/L$ where z is the coordinate along the fiber axis and L is the cavity length. $T = t(\beta'' L)^{-1/2}$ where t is the time coordinate in a reference frame traveling at the group velocity of light and β'' is the dispersion coefficient. $E_{\pm} = (\gamma L)^{1/2} A_{\pm}$ where $A_{\pm}$ is the electric field amplitude and $\gamma = 2n_2\omega(cA_{\text{eff}})^{-1}$, n_2 being the nonlinear index coefficient and A_{eff} the effective fiber core area. Note that in accordance with the sign of the second derivative in Eq. (1), we only consider the normal dispersion regime. This allows us to avoid the detrimental effect of the temporal symmetry breaking instability that would lead to uncontrollable changes in the pulse peak positions [16].

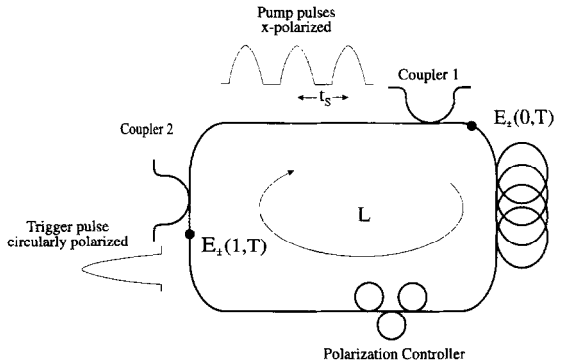

Fig. 1. Schematic of the nonlinear passive fiber ring cavity proposed as polarization based all-optical memory.

The cavity field dynamics are completed by the following cavity boundary conditions:

$$E_{\pm}^{n+1}(Z=0,T) = \theta E^{\text{in}}(T) + \rho^2 \exp(-i\Delta\theta^2)\, E_{\pm}^n(Z=1,T) \qquad (2)$$

where θ and ρ are the amplitude transmission and reflection coefficients of the couplers ($\rho^2 + \theta^2 = 1$). $E^{\text{in}}(T)$ represents the normalized equal circular polarization components of the linearly polarized pump wave. The quantity $\phi_0 = \Delta\theta^2$ is the linear phase detuning of the cavity. For simplicity, the detuning is described in the following by the scaled detuning parameter $\Delta = \phi_0\theta^{-2}$, where θ^2 represents the loss of the cavity. In the good cavity limit θ^2 is

inversely proportional to the finesse of the cavity and Δ thus gives the deviation from resonance in terms of resonance widths. This allows us to quantify the detuning independently of the finesse. Iterating the map (2) requires numerical integration of the coupled NLS equations (1). To this end we used a standard split-step Fourier algorithm.

In the case of cw excitation it is well known that the steady-state linearly polarized (scalar approximation) solutions of map (2) exhibit optical bistability [5]. Areshev and coworkers [19] found, in the equivalent spatial problem with linearly polarized plane wave excitation, the existence of a symmetry-breaking bifurcation characterized by the appearance of branches of elliptically polarized steady-state solutions, underlining that optical bistability description in nonlinear resonators without taking into consideration polarization results insufficient.

Fig. 2 shows the cavity steady-solutions obtained iterating Eqs. (1) and (2) with cw input excitation $\theta^2 = 0.05$ and $\Delta = 4$. Besides optical bistability, symmetry-breaking appears as a pitchfork bifurcation of the linearly polarized (that is, symmetric) solution. At the bifurcation point, the linearly polarized solution exchanges its stability (with respect to cw perturbations) with two new stable elliptically polarized solutions, with the same ellipticity and opposite handedness. Ref. [17] presents, through a mean-field description of our device, a simple analysis of this bifurcation with cw input excitation. In particular, it is showed that the polarization symmetry-breaking bifurcation requires a detuning Δ greater than $(3)^{1/2}$ (which in turn implies a scalar bistable response) and analytical expressions are obtained for the threshold intensity $X_{\mathrm{cw,bif}}$.

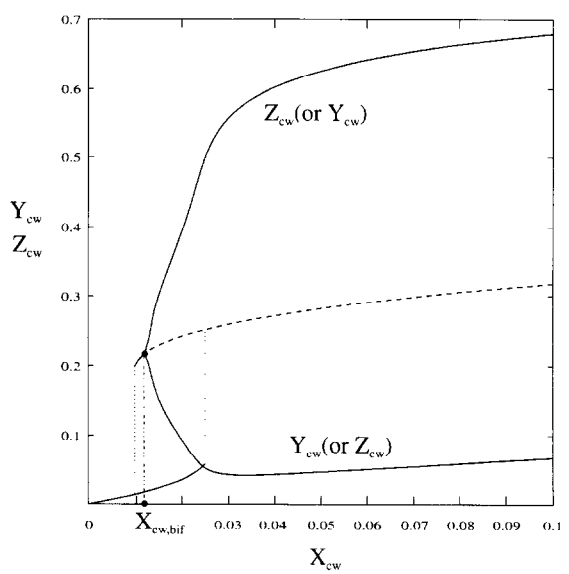

Fig. 2. Steady-state responses obtained with linearly polarized cw input pump. Besides the bistable loop, a symmetry-breaking pitchfork bifurcation appears with elliptically polarized states with the same ellipticity (defined as $\pm\tan(b_s/a_s)$ where b_s and a_s are the short and long axes of the polarization ellipse) and opposite handedness. Dashed curves correspond to unstable symmetric (linearly polarized) states. The cavity parameters are $\Delta = 4$ and $\theta^2 = 0.05$.

In the following section we show that polarization symmetry-breaking bifurcation still exists in the case of synchronous pulsed excitation.

3. Polarization symmetry-breaking and flip-flop operation

Let us first consider the presence of the pump wave alone in the cavity. We assume that the pump wave is composed of ideal transform-limited linearly polarized sech pulses which we note $E^{\mathrm{in}} = X_p^{1/2}\mathrm{sech}(T/T_0)$ where X_p is the normalized input peak power and T_0 the normalized pulse duration. Fig. 3(a) shows the obtained response of the cavity to the periodic pump. It shows the peak power of each polarization component of the cavity pulses $Y_p = |E_+(Z=0,T=0)|^2$ and $Z_p = |E_-(0,0)|^2$ versus the input power X_p for the following dimensionless parameters: pulse duration $T_0 = 10$, cavity detuning $\Delta = 4$, and cavity loss $\theta^2 = 0.05$. As can be seen, at low input peak power the cavity response curve exhibits the usual scalar bistable cycle [16] where the two circular components are equal ($Y_p = Z_p$). However, for input peak power greater than a threshold $X_{\mathrm{p,bif}}$, a polarization symmetry-breaking bifurcation clearly appears: the linearly polarized state becomes unstable and the field switches to either a right-handed or left-handed elliptical polarization state. The pulse profiles corresponding to the stable asymmetric branch are shown in Fig. 3(b) for $X_p = 0.078$, a value greater than $X_{\mathrm{p,bif}}$. Note that both pulses have the same total intensity. In Figs. 3(c), 3(d) we plot the parameters of the corresponding polarization states. We show that locally both states have the same ellipticity but opposite handedness.

This behavior has been observed over a wide range of parameters. Numerous simulations performed for values of T_0 ranging from 1 to 20 have led to qualitatively similar results. We have observed however that the shorter the pulse width the larger the bifurcation intensity $X_{\mathrm{p,bif}}$. This is graphically shown in Fig. 4 for the same cavity parameters than Fig. 3(a). The threshold intensity for $T_0 = 2$ becomes an order of magnitude higher than with cw input. We have also verified that the symmetry breaking does not depend critically on the cavity finesse. It has been observed for cavity losses as high as 0.3. These results suggest that the polarization symmetry breaking would occur in many practical situations and that its application to optical storage is worth investigating.

The proposed storage device uses the possibility to switch the polarization state of the cavity pulses from one asymmetric branch to the other. One way of performing

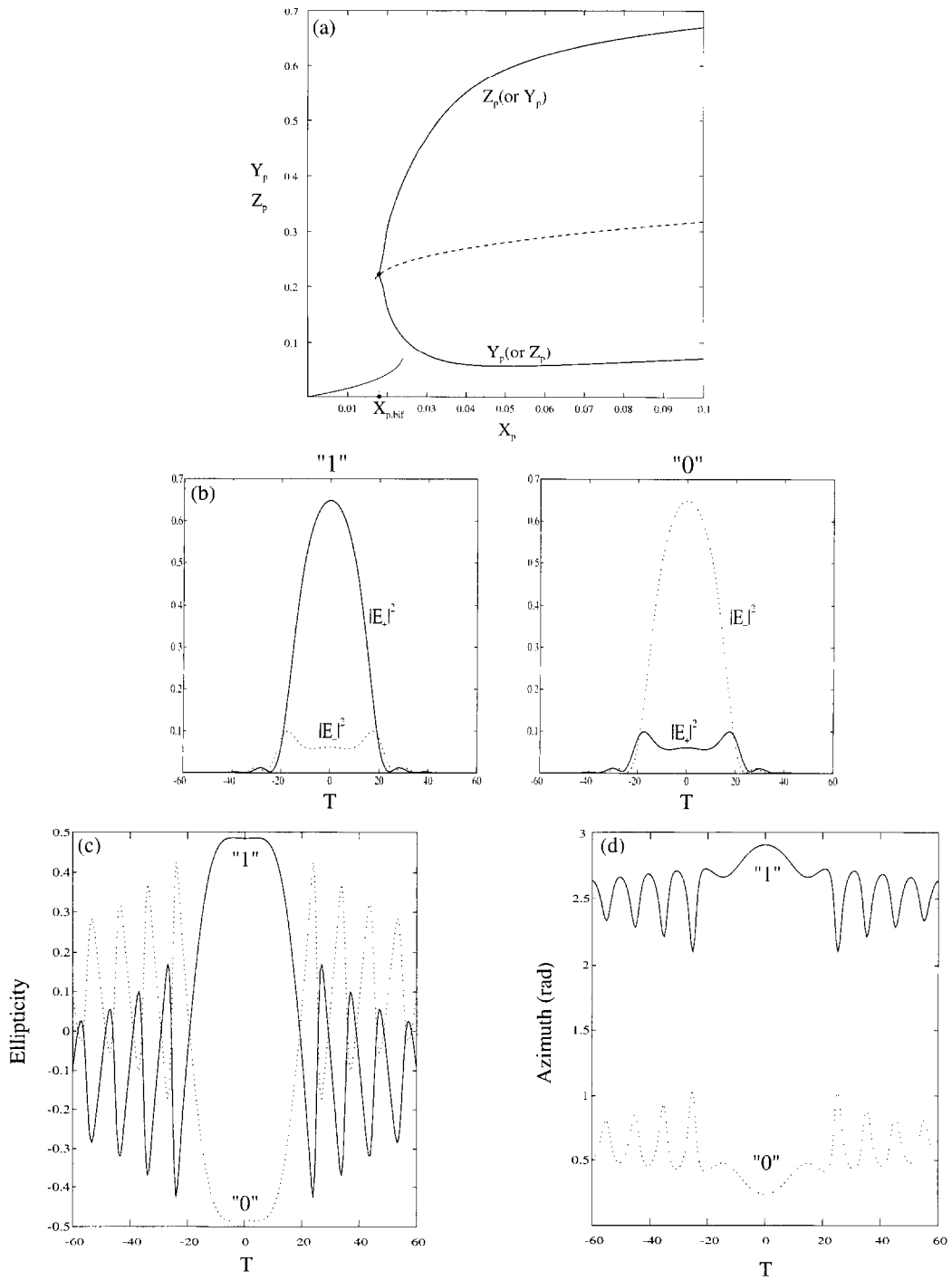

Fig. 3. (a) Steady-state curves obtained for the cavity pulse peak intensity Y_p and Z_p versus the symmetric pulsed input $X_{p+} = X_{p-} = X_p$. The bistable loop and the asymmetric solutions are shown. Dashed curves correspond to the unstable symmetric states. The parameters are $\Delta = 4$, $T_0 = 10$ and $\rho^2 = 0.95$, with no birefringence. (b) Power profiles of the two steady asymmetrical cavity-pulses (''1'' and ''0'' of the memory proposed) corresponding to $X_p = 0.078$ in (a). They have the same total intensity and only different polarization features. (c), (d) Ellipticity and azimuth of the polarization ellipse corresponding to the two above asymmetrical cavity-pulses.

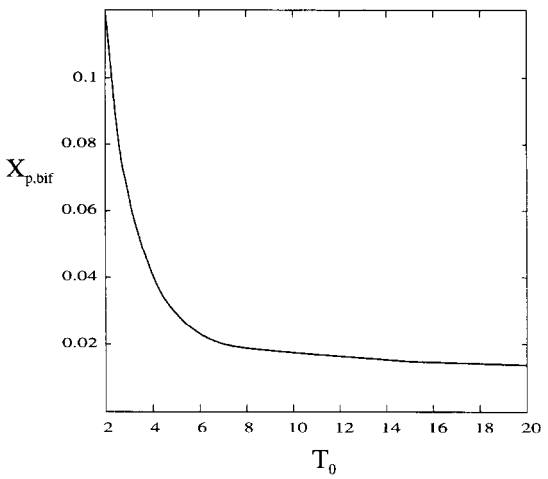

Fig. 4. Influence of the input pulse width on the threshold intensity of the symmetry-breaking bifurcation with the same parameters as in Fig. 3(a). The increase of $X_{p,bif}$ for shorter input pulses is evidenced. The curve tends to the cw threshold intensity value as T_0 goes to infinity.

such a switching is simply to increase selectively the intensity of one of the polarization components of the pump pulses. This increase would break the balance between the opposite circular polarizations and would force the cavity pulses to take the dominating polarization. The way in which switching occurs is illustrated in Fig. 5 where we plot the cavity pulse intensities Y_p and Z_p as a function of the power of one of the input pulse components, say, X_{p+}, for a fixed value of the power of the other which we choose above the bifurcation point, $X_{p-} = 0.078$.

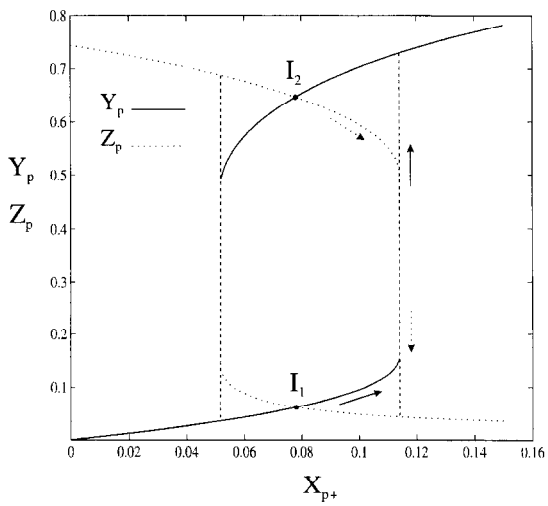

Fig. 5. Interleaved response curves of Y_p and Z_p versus X_{p+} with the same parameters as in Fig. 3(a). The fixed left circular input intensity $X_{p-} = 0.078$ is chosen above the bifurcation point. The increase of the right circular intensity induces switching of the right circular power from I_1 to I_2 and the left one from I_2 to I_1.

The response curves take the form of two interleaved hysteresis cycles. The two intersecting points I_1, I_2 correspond to the lower and upper asymmetric branches of Fig. 3(a) for $X_p = 0.078$, respectively. If the right circular intensity of the cavity pulse is initially on the lower branch (point I_1), a trigger pulse added to this polarization component in the pump field will make this polarization follow the bistable hysteresis cycle and switch to the upper branch (point I_2). In the meantime the left polarization component, which was initially on the upper branch (point I_2), has switched towards the lower branch (point I_1). Naturally this operation can be repeated with the other polarization component to reset the system to its initial state. This simple reasoning shows that set-reset flip-flop operations can be performed in the fiber ring, which then appears as a potentially interesting device for all-optical storage applications.

Although this way of performing flip-flop operation seems natural from Fig. 5, it is not practical. In fact the characteristic switching times of the hysteresis cycles of Fig. 5 are of the order of the cavity build-up time. This implies that the trigger pulse for the switching of a given bit must be hold on during several round-trips. Operations on individual bits are therefore slow and relatively complex. To avoid this difficulty the polarization state of the pulses should be switched within the cavity. Ideally, one could use an ultrafast all-optical nonlinear polarization switching element in the cavity in order to perform flip-flop operation on the time scale of the pulses duration. Here, we study a simpler technique: we consider triggering by injection in the cavity of polarized pulses of large intensity. As we shall see below, such injection forces the cavity pulses to take the polarization of the trigger pulses and allows therefore for flip-flop operations.

Fig. 6 illustrates the switching dynamics obtained with this triggering technique. It shows the pulse peak intensities Y_p and Z_p of both polarization components within the cavity as a function of the number of round-trips. The

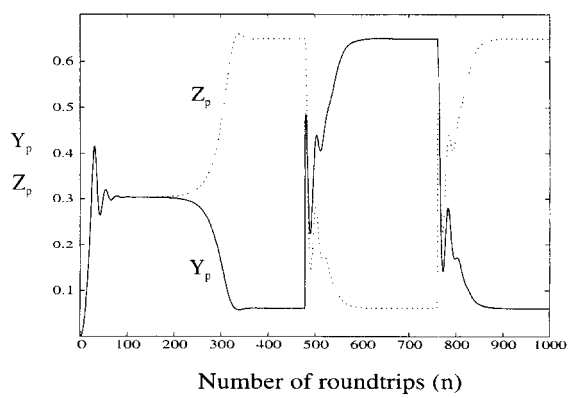

Fig. 6. Illustration, through the dynamics of the peak powers, of the flip-flop operation of a single pulse in the cavity. Same parameters as in Fig. 3(a) with $X_p = 0.078$ and cavity trigger amplitudes $E_{\pm} = 0.56$.

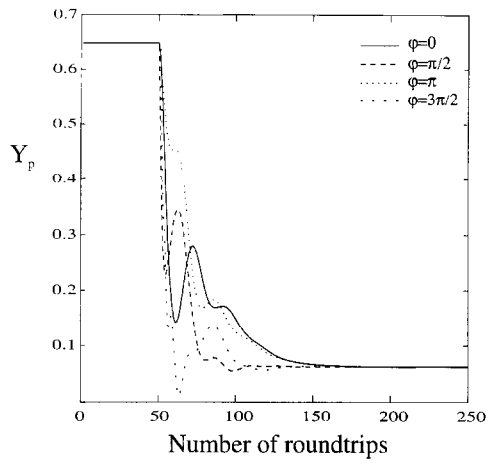

Fig. 7. Transient dynamics showing switching for some values of phase differences between trigger and pump pulses, $\varphi \in [0, 2\pi)$. Down-switching is obtained for any value of φ with an adequate trigger amplitude. The amplitude values of the circular left-handed triggers are $E_- = 0.56$ ($\varphi = 0$ and $3\pi/2$), $E_- = 1.19$ ($\varphi = \pi/2$) and $E_- = 0.69$ ($\varphi = \pi$).

parameters are those considered in Fig. 3. The first part of the curve corresponds to the initialization of the system. The pump intensity X_p is increased abruptly beyond the bifurcation point up to $X_p = 0.078$. As can be seen in Fig. 6, after damped oscillations the system reaches the unstable symmetric state. Due to small perturbations initially seeded, the symmetry is broken and the system tends to one of the stable asymmetric states of Fig. 3. With our convention this state corresponds to a low intensity in the right-handed polarization component (point I_1 in Fig. 5 or "0" in Fig. 3(b)). Once the steady state is established, a single trigger pulse is injected in the cavity with a purely circular right-handed polarization, an amplitude of $E_+ = 0.56$ and same width as the input. As can be seen, under the effect of the trigger pulse, the polarization state swaps from one stable asymmetric state to the other. Lower amplitude values of the trigger do not lead to switching. After the transient a second trigger pulse is added to the system with a left-handed polarization in order to reset the system to its initial state. Hence, a complete cycle of set-reset type flip-flop operation is accomplished.

The influence of the phase relationship between the trigger pulse and the input cavity field has been investigated. We have considered circularly polarized trigger pulses of the form $E_{trig} = X_{p,trig}^{1/2}\ \mathrm{sech}(T/T_0)\ \exp(i\varphi)$ with $X_{p,trig}^{1/2}$ the peak amplitude and φ the phase difference between the trigger and input pulses, ranging from 0 to 2π. We have verified that up and down switching can be produced with any value of φ just taking an appropriate trigger amplitude. Fig. 7 shows the transient dynamics with some phase differences evidencing down-switching in all cases.

4. Memory operation

The above study of polarization switching in the fiber loop has been performed by numerical simulations of the propagation of a single isolated pulse synchronously pumped in the cavity. In order to assess the usefulness of the studied processes for application to optical storage, it is necessary to investigate the dynamics of pulse trains in the cavity. Pulses in these trains must be addressable independently in order to store information in the cavity. The capacity of a fiber loop memory is strongly dependent on the allowed pulse spacing. It is therefore important to study pulse interaction in the cavity. This is the aim of the present section.

We performed numerical simulations on packets of eight pulses. Fig. 8 illustrates switching operations using the trigger mechanism studied above, it is representative of our simulations. It shows in the form of contour lines, the intensity of one of the polarization components (by convention, the predominantly right-handed polarized pulse associated with bit "1"). The cavity parameters are those of Fig. 6 and the input pulse separation is 5 times the pulse width. The system is initialized with a uniform sequence of eight bits "1". A left-handed trigger pulse is launched in

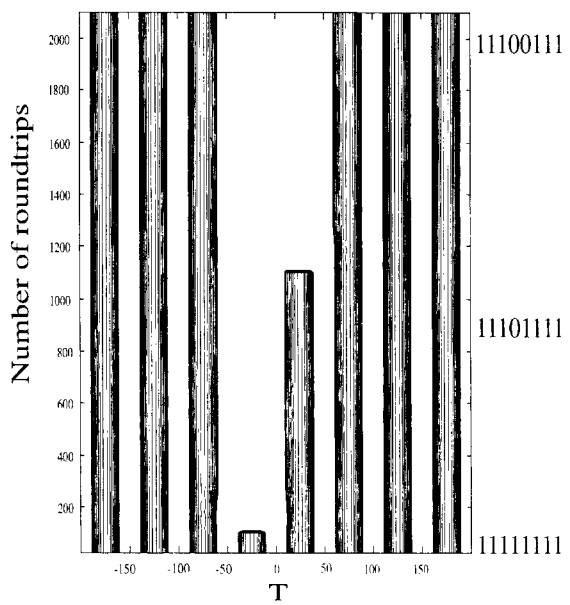

Fig. 8. Illustration of erasing (or writing) operations of individual bits. The stability of the bit patterns through several roundtrips is shown. The eight cavity-pulses initially represent the periodic binary code ...11111111... After the first trigger launched, the bit packet stored becomes ...11101111..., and finally, with the addition of another trigger, we switch to ...11100111... To clarify the switching dynamics, contour lines are plotted only for the highest intensities. The simulation is performed with $X_p = 0.078$, $\Delta = 4$, $T_0 = 10$, $\rho^2 = 0.95$ and pulse separation of 5 times the pulse width.

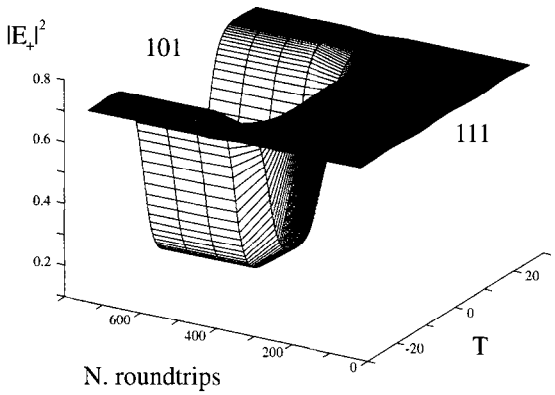

Fig. 9. Switching of one bit from "1" to "0" while the surrounding bits remain unchanged for a minimum pulse separation of 2 times the pulse width. Same parameters as in Fig. 8.

the fourth time slot in order to switch the corresponding bit to "0". After the transient another left-handed trigger pulse is used now to switch the fifth bit to "0". This simulation clearly shows that erasing (or writing if we consider the predominantly left-handed steady pulse as the "1") can be performed independently on each pulse of the bit pattern. Our numerical experiments have also shown that flip-flop operation (i.e. erasing and writing on the same time slot) can be accomplished on individual bits of the stored pattern. The separation between the pulses in the bit string can be decreased to a minimum of 2 times the pulse width. This is illustrated in Fig. 9 where we show the switching of one bit from "1" to "0" while the surrounding bits remain unchanged. Note that contrary to the usual fiber loop storage devices, the bit patterns in the synchronously pumped cavity do not need timing stabilization techniques, the stability of the pulse position being provided by the synchronous periodic pumping.

Because the principle of operation of the proposed device is based on polarization dynamics, it is essential to investigate the behavior of the system in the presence of birefringence in the fiber. In practice, residual or stress-induced birefringence is unavoidable in optical fibers and to be realistic our model should account for it. When considering weak birefringence the coupled NLS equations describing pulse propagation in the cavity become [20]:

$$\frac{\partial E_{\pm}^{n}}{\partial Z} = -\frac{\mathrm{i}}{2}\frac{\partial^2 E_{\pm}^{n}}{\partial T^2} + \mathrm{i}\left(\tfrac{1}{3}\left|E_{\pm}^{n}\right|^2 + \tfrac{2}{3}\left|E_{\mp}^{n}\right|^2\right)E_{\pm}^{n} + \mathrm{i}\kappa E_{\mp}^{n} \pm \mathrm{i}\delta E_{\pm}^{n}, \tag{3}$$

where κ and δ respectively are the scaled linear and twist induced circular birefringence coefficients given by $\kappa = (\beta_x - \beta_y)L/2$ and $\delta = 0.08\xi L$ with ξ the number of twists per unit length [21]. Let us first consider the presence of linear birefringence only. In this case the birefringent terms in Eq. (3) do not break the symmetry of the system. Accordingly, numerical simulations have shown

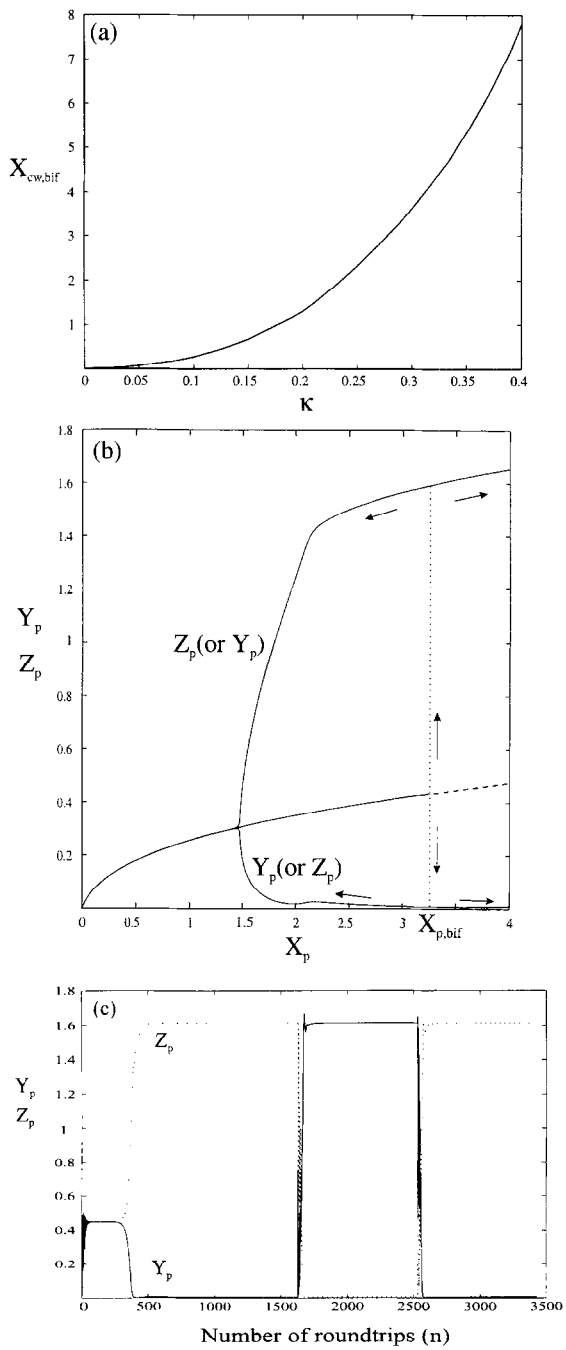

Fig. 10. (a) Influence of the linear birefringence on the threshold bifurcation intensity for cw input. Same parameters as in Fig. 2. Similar dependence is obtained with pulsed input. (b) Steady-state responses obtained with synchronously pulsed pump, weak linear birefringence ($\kappa = 0.4$, $\delta = 0$) and $\Delta = 4$, $T_0 = 10$ and $\rho^2 = 0.95$. The bifurcation presents threshold bifurcation intensity two orders of magnitude higher than without anisotropy, Fig. 3(a). Moreover, bistability appears between the symmetric and asymmetric branches. (c) Flip-flop operation is shown to be possible with $X_p = 3.5$.

that symmetry breaking still occurs in cw and pulsed regime. However, the threshold intensity for symmetry-breaking bifurcation is extremely dependent on the birefringence. This is presented in Fig. 10(a) for cw input excitation, $\Delta = 4$ and $\theta^2 = 0.05$. An equivalent dependence is obtained with synchronously pulsed pump. Owing to the high input intensities required to operate the device in the symmetry-breaking domain, stable flip-flop operations can only be performed with birefringence sufficiently small. As a general rule, the birefringence must be $\Delta n \leq 10^{-7}$ for fiber loop lengths of the order of a few meters. Such a low birefringence can be obtained in especially designed fibers such as the so-called spun fibers [21]. As illustrated in Fig. 10(b) for pulsed input, the symmetry-breaking bifurcation presents a threshold intensity two orders of magnitude higher than without birefringence and bistability appears between the asymmetric and symmetric branches. Fig. 10(c) illustrates flip-flop operations in the conditions of Fig. 10(b).

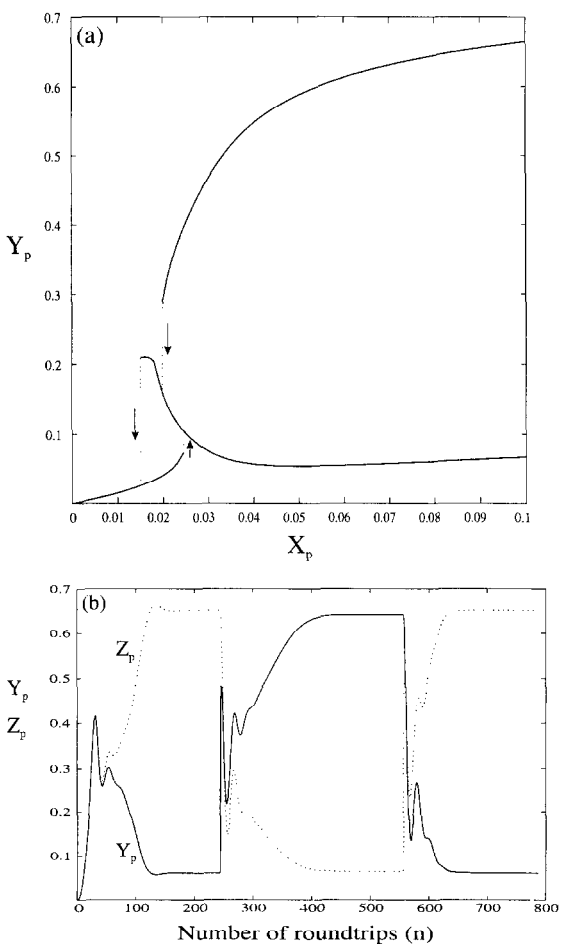

Fig. 11. (a) Pulsed steady-state curves obtained with low circular birefringence ($\delta = 10^{-3}$, $\kappa = 0$). For clarity, only the right-handed polarization is shown. (b) Flip-flop operation is shown to be possible with $X_p = 0.078$.

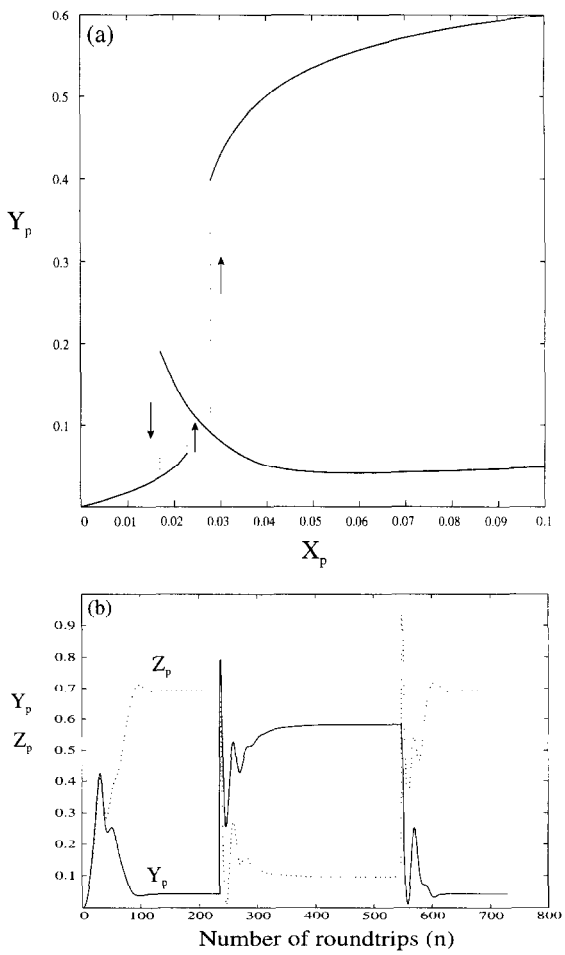

Fig. 12. (a) Pulsed steady-states curves obtained with a strong twisting in the fiber, $\delta = 2\pi$, and weak linear birefringence $\kappa = 0.4$. For clarity, only the right-handed polarization is plotted. The averaging of the linear birefringence to zero and the approximated validity of the isotropic model of Eqs. (1) and (2) is shown. (b) Illustration of flip-flop operation with $X_p = 0.078$.

In the presence of circular birefringence, the terms $\pm i\delta E_{\pm}$ must be considered in Eq. (3). These terms clearly break the symmetry of the equations and the symmetry-breaking bifurcation can no longer be observed. However, in the case of low circular birefringence the cavity still exhibits multi-valued transmission curves. They are shown in Fig. 11 for the same parameters as those of Fig. 3(a) but with a circular birefringence coefficient of $\delta = 10^{-3}$. The curves are clearly reminiscent of the symmetry-breaking bifurcation and, as shown in Fig. 11(b), flip-flop operation is still possible. This behavior has been observed for values of δ up to $\delta = 10^{-2}$. Note that circular birefringence can be controlled by applying a twist to the fiber. Twisting the fiber may therefore be used to compensate for residual circular birefringence in order to obtain values of δ compatible with flip-flop operations.

Let us point out that twist-induced circular birefringence provides a way to recover the isotropic model. If the applied twist is strong, the resulting circular birefringence induces an averaging of the linear birefringence to zero and can therefore be neglected, which makes valid our model with Eqs. (1) and (2). This averaging effect can be easily understood from the following reasoning: Applying the change of variables $E_{\pm} = F_{\pm}\exp(\pm i\delta Z)$, the terms in δ disappear in Eq. (3) and the linear birefringence terms become $i\kappa \exp(\mp 2i\delta Z)F_{\mp}$. Assuming strong twisting, the corresponding large value of δ will induce fast oscillations of these terms. Integration of Eq. (3) will then average them to zero and Eq. (3) become identical to Eq. (1). Naturally, in order to keep the same boundary conditions, Eq. (2), the twisting must be controlled such that the same detuning is obtained in both polarization components. In other terms, δ must be a multiple of π. This condition can be obtained by means of a polarization controller in a way analogous to what was done in previous fiber cavity experiments [22]. Fig. 12(a) shows the obtained results for the same parameters of Fig. 3(a), but $\kappa = 0.4$ and $\delta = 2\pi$. Flip-flop operation is shown in Fig. 12(b) for the birefringent conditions of Fig. 12(a). This brief analysis of birefringence effects suggests that flip-flop operations seem possible in practical nonlinear fiber loops.

5. Discussion and conclusion

In conclusion, we have investigated the possibility of realizing a passive all-optical fiber loop memory based on polarization dynamics. The principle of operation is based on a polarization symmetry-breaking bifurcation. This feature allows for set-reset flip-flop mode of operation which constitutes a significant advantage with respect to usual fiber loop storage devices. Another advantage of the proposed device is the high potential bit density. Due to the good stability of the system the pulses can be packed at a high density. The maximum number of bits that can be stored in the cavity is $N_{\text{bits}} \simeq t_R/[\tau T_0(\beta'' L)^{1/2}]$, where τ is the ratio between the pulse spacing and the pulse width. We choose here $\tau = 2$ as in the illustration of Fig. 6. For a fiber length of 1 m, a cavity loss of $\theta^2 = 0.05$, a normal dispersion of 10 ps^2/km, and an input pulse width of $T_0 = 10$ which corresponds in real units to 1 ps, the roundtrip time is approximately 5 ns and the number of stored bits is 2.5×10^3. This value corresponds to a bit rate of 500 Gb/s. This bit rate is the rate at which the pump pulses have to be supplied and is thus also the rate at which the "read-out" of information stored is delivered. Another important parameter is the rate at which information can be processed. Typically the time for a bit to be encoded is around $100t_R$. Thus, the maximum information processing rate (IPR), i.e. the number of bits encoded by unit of time is 2.5×10^3 bits/500 ns = 5 Gb/s, assuming that every bit in the circulating binary string is required to be changed. On the other hand, if only one bit in the string is required to be changed then the IPR drops to 1 bit/500 ns = 2 Mb/s.

The above physical conditions correspond to the following power requirements: if we consider a wavelength of 800 nm with nonlinear coefficient $\gamma = 60\ km^{-1}\ W^{-1}$ [23], the bias intensity $X_p = 0.078$ corresponds then to a peak power of approximately 2.5 W, and the cavity pulse peak power is of the order of 10 W, while the value of the trigger pulse peak power in the cavity is 5 W.

The stability of the synchronous and coherent pumping is another important issue to be addressed. In the theory presented above, we considered that the cavity phase detuning has a given constant value. In order to obtain such a condition in practice, the cavity length must be interferometrically stabilized. This can be performed by means of the technique proposed by Reynaud et al. [24] in which interferometric stabilization with an accuracy of $\lambda/200$ of fiber lengths of several tens of meters has been described. As a matter of fact, on the basis of this technique we are now making an experiment [25] on the scalar version of the nonlinear fiber loop presented here. Results indicate that cavity length stabilization can be performed at an accuracy of $\lambda/200$ using a picosecond mode-locked Ti-Sapphire laser. Note that the principle of operation of the proposed flip-flop memory can be used in other systems exhibiting a polarization symmetry-breaking bifurcation. For instance, a spatial memory could be realized in the so-called Λ-system [26]. This device consists of a Fabry-Pérot cavity filled with a two-level atomic vapor. A polarization symmetry-breaking similar to that described here for silica fibers has been observed experimentally in this system.

Acknowledgements

The work of J.G.M. was partially supported by the Spanish DGCYT under grant AP92-40985447, the HCM contract CHRX-CT93-0382 and the Universitat Politècnica de Catalunya (UPC). The work of M.H. was partially supported by the Inter-University Attraction Pole Program of the Belgian Government under grant P3-047 and the Belgian National Fund for Scientific Research. J.G.M. gratefully acknowledges the hospitality of all the members of the Service d'Optique et Acoustique of the Université Libre de Bruxelles (ULB) over several visits, helpful discussions with J.P. Torres from the UPC and some computational resources generously offered by L. Torner. We acknowledge constructive comments made by one of the reviewers.

References

[1] V.I. Belotitskii, E.A. Kuzin, M.P. Petrov and V.V. Spirin, Electron. Lett. 29 (1993) 49.

[2] H. Avramopoulos and N.A. Whitaker, Optics Lett. 18 (1993) 22.
[3] C.R. Doerr, W.S. Wong, H.A. Haus and E.P. Ippen, Optics Lett. 19 (1994) 1747.
[4] J.D. Moores, K.L. Hall, S.M. LePage, K.A. Rauschenbach, W.S. Wong, H.A. Haus and E.P. Ippen, IEEE Photonics Tech. Lett. 7 (1995) 1096; K.L. Hall, J.D. Moores, K.A. Rauschenbach, W.S. Wong, E.P. Ippen and H.A. Haus, IEEE Photonics Tech. Lett. 7 (1995) 1093.
[5] J.V. Moloney, Phys. Rev A 33 (1986) 4061.
[6] H.M. Gibbs, Optical bistability: controlling light with light (Academic Press, 1985).
[7] A.E. Kaplan and P. Meystre, Optics Comm. 40 (1982) 229.
[8] K. Otsuka, Optics Lett. 14 (1989) 72.
[9] M. Haelterman and P. Mandel, Optics Lett. 15 (1990) 1412.
[10] K. Otsuka, Electron. Lett. 24 (1988) 800.
[11] M. Haelterman, Optics Comm. 86 (1991) 189.
[12] J. Danckaert and G. Vitrant, J. Appl. Phys. 71 (1992) 6204.
[13] K.P. Panajotov, T. Tenev, G. Zartov, M. Pelt, J. Danckaert, H. Thienpont and I. Veretennicoff, J. Nonlinear Opt. Phys. Mater. 5 (1996) 351.
[14] H. Thienpont, J. Danckaert and I. Veretennicoff, Pure Appl. Optics 2 (1993) 515.
[15] G.S. McDonald and W.J. Firth, J. Opt. Soc. Am. B 6 (1989) 1736; J. Opt. Soc. Am. B 10 (1993) 1081.
[16] M. Haelterman, G. Vitrant and J. García-Mateos, in: Nonlinear Waveguides and Their Applications, Vol. 6, 1996 OSA Technical Digest Series (Optical Society of America, Washington DC, 1995) pp. 201–203; J. García-Mateos, F. Canal and M. Haelterman, Fiber Integrated Optics 14 (1995) 337.
[17] M. Haelterman, S. Trillo and S. Wabnitz, J. Opt. Soc. Am. B 11 (1994) 446.
[18] S. Trillo and S. Wabnitz, J. Opt. Soc. Am. B 6 (1989) 238.
[19] I.P. Areshev, T.A. Murina, N.N. Rosanov and V.K. Subashiev, Optics Comm. 47 (1983) 414.
[20] S. Trillo, E.M. Wright and G.I. Stegeman, Optics Comm. 70 (1989) 166.
[21] A.J. Barlow, J.J. Ramskov-Hansen and D.N. Payne, Appl. Optics 20 (1981) 2962.
[22] R. Vallée, Optics Comm. 81 (1991) 419.
[23] G.P. Agrawal, Nonlinear fiber optics, 2nd Ed. (Academic Press, 1995).
[24] F. Reynaud and E. Delaire, Electron. Lett. 29 (1993) 1718.
[25] S. Coen, M. Haelterman, Ph. Emplit, L. Delage and F. Reynaud, in: Nonlinear Guided Waves and Their Applications, Vol. 15, 1996 OSA Technical Digest Series (Optical Society of America, Washington DC, 1996) pp. 173–175.
[26] M. Kitano, T. Yabuzaki and T. Ogawa, Phys. Rev. Lett. 46 (1981) 926.